- *Technical Paper* -

AN EXPERIMENTAL INVESTIGATION ON THE CYCLIC BEHAVIOUR OF FERRO-CEMENT LAMINATED MASONRY INFILLED RC FRAME

Debasish SEN[*1], Yuta TORIHATA[*1], Hamood ALWASHALI[*2], and Masaki MAEDA[*3]

ABSTRACT

In developing countries, Ferro-cement lamination on masonry would be a low cost solution for strengthening of RC buildings. This study aims to investigate the seismic performance of two half-scaled masonry infilled RC frames, without and with Ferro-cement lamination on masonry. The experimental results showed that Ferro-cement could help in increasing the lateral strength about two times. Simple prediction model has been investigated and it could estimate the strength of Ferro-cement laminated infilled frame. In addition, Ferro-cement technique showed good energy dissipation than infilled masonry.

Keywords: RC frame, Ferro-cement, Wire mesh, Masonry infill, Seismic strengthening.

1. INTRODUCTION

Seismic strengthening of existing RC buildings is of utmost important for structural engineers, especially in developing countries because of the limitation of capital and expertise. In developing countries, strengthening of existing building component would be more viable than insertion of additional structural element e.g. shear wall, steel bracing etc. Sometimes, RC buildings contain masonry infill as partition wall because of the availability of ingredients locally. However, masonry walls are considered as non-structural elements in most of the building design codes. Strengthening of existing infilled masonry, to convert them as structural element, would be one of the probable candidate to utilize existing component of building for strengthening purpose. Some reinforcing material and connection with surrounding RC frame are required to make existing infilled masonry to structural element. In this context, Ferro-cement (FC) lamination, Textile mortar reinforcement (TRM), Fiber reinforced mortar etc. are probable candidates for masonry strengthening. Among these methods, Ferro-cement lamination is low cost, can be easily applied and low labor intensive, which is feasible for developing countries. In general, Ferro-cement retrofitting of masonry refers to the application of an initial mortar layer on the both faces of masonry wall which is followed by the placement of steel wire mesh and a second mortar layer. Some anchorages are also being used to attach wire mesh to masonry and RC frame as shown in Fig. 1. Though, Ferro-cement has been studied for decades as a construction material, there is no design specification i.e. amount of mesh reinforcement under lateral loads. ACI-549 [1] also addressed the lacking of study on the Ferro-cement under lateral force. As a part of SATREPS-TSUIB project in Bangladesh (https://www.satreps-tsuib.net/), which is sponsored by JST, authors are trying to develop an effective way to retrofit existing infill masonry with Ferro-cement lamination as a low cost and less labour intensive strengthening method for developing countries.

The objective of this study is to experimentally investigate the effect of Ferro-cement lamination on the lateral strength, energy dissipation and failure mode of masonry infilled RC frame.

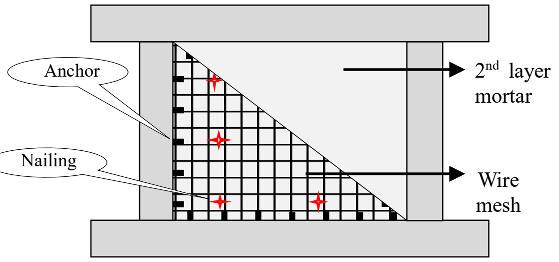

Fig. 1 Schematic diagram of FC lamination on masonry infill

2. LITERATURE REVIEW

In this study, primarily experimental results of several half scaled masonry infilled RC frames, with and without Ferro-cement retrofitting, have been acquired from literature [2-8] to get an idea about the practices in research field. All the studied FC laminated masonry walls contain square wire mesh on solid or hollow bricks. The lateral contribution of Ferro-cement layer has been determined from the difference in lateral capacity of retrofitted and without retrofitted specimens. Afterward, the shear stress on FC lamination (τ_{FC}) has been computed considering cross sectional area of FC laminate. The in-plane shear stress on Ferro-cement laminate is presented in Fig. 2 as a function of normalized horizontal mesh reinforcement area (A_{hs}/A_{mas}), where A_{hs} = total area of horizontal mesh reinforcement and A_{mas} = horizontal cross sectional area of masonry. From Fig. 2, the horizontal mesh reinforcement varies between 0.05~0.8% of the horizontal masonry area. The shear stress on FC layer varied greatly between specimens.

*1 Graduate School of Engineering, Tohoku University, JCI Student Member
*2 Assistant Prof., Dept. of Architecture and Building Science, Tohoku University, Dr.E., JCI Member
*3 Professor, Dept. of Architecture and Building Science, Tohoku University, Dr.E., JCI Member

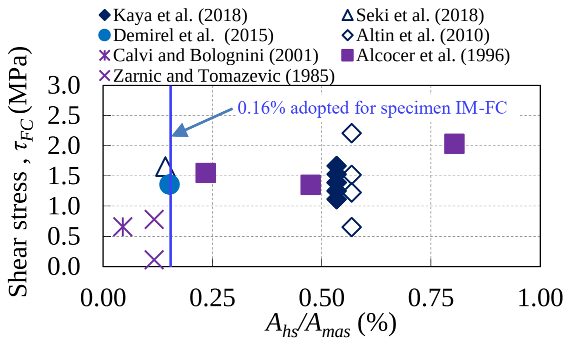

Fig. 2 Shear strength of FC layer as a function of mesh reinforcement ratio

This large variation in past experimental results could be due to varying materials types and connections of Ferro-cement layer with the surrounding RC frame.

3. EXPERIMENTAL PROGRAM

There is no guideline for the amount of mesh reinforcement required for Ferro-cement lamination of infilled masonry. In this study, the lower boundary of mesh reinforcement ratio from literature survey has been focused and set to be 0.16% of horizontal masonry area.

3.1 Specimen Details

Two half scaled masonry infilled RC frames, without and with Ferro-cement layer, have been considered with relatively weak column to focus on the field practice in Bangladesh. The details of both specimens are shown in Table 1. The control infilled masonry specimen (IM) has been adopted from Alwashali et al. [9]. The Ferro-cement laminated specimen (IM-FC) has the same geometric configuration and material composition as the control specimen (IM). The overall geometry of RC frame is shown in Fig. 3(a). After construction of RC frame, masonry panel has been built in frame, with solid bricks of 210x100x60 mm in running bond manner. The gap between top brick layer and the upper beam has been carefully filled up with mortar. After seven days of masonry construction, 10mm thick mortar has been mounted on the both faces of masonry wall. This is followed by the attachment of square wire mesh to the RC frame and masonry wall. The wire mesh has been connected to surrounding RC frame with bolt (inserted into pre-installed thread) and steel plate as shown in Fig. 3(b). In addition, the wire mesh has been connected with masonry infill by 32mm nails to hold the wire mesh in place during application of second layer mortar. The nails have been placed in drilled holes at a horizontal and vertical center to center distance of 250mm and 500mm, respectively. Epoxy has been used to attach the nail with masonry. After seven days, the second layer of mortar with thickness of 15mm has been applied on wire mesh.

3.2 Materials properties

The material tests were conducted for each specimen individually and simultaneously with the frame loading. The mechanical properties of concrete, reinforcing steel, and masonry are shown in Table 2, Table 3, and Table 4, respectively. The concrete, used

Table 1 Details of specimen

Spec-imen	RC column (mm)	Wire mesh: Wire diameter (mm)	Spacing (mm)	Mesh ratio (%)
IM	200x200	-	-	-
IM-FC	200x200	0.9	5.45	0.16

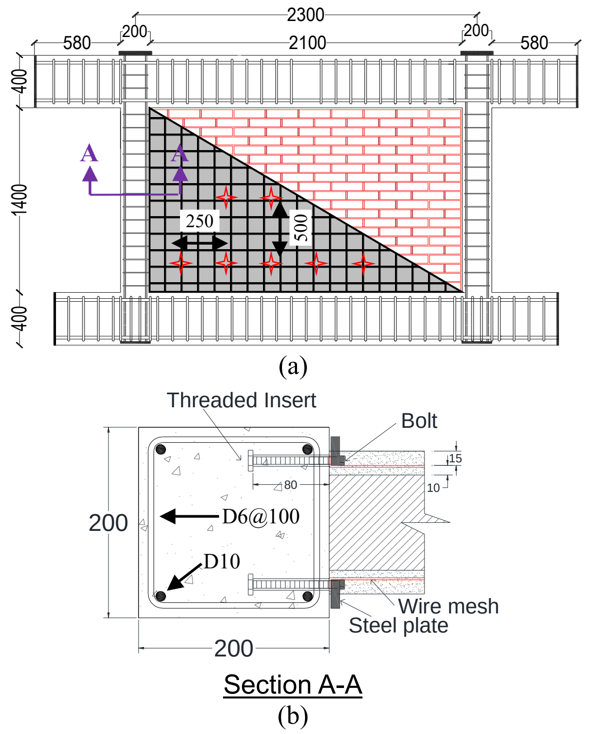

Fig. 3 (a) Geometry of masonry infilled RC frame (b) connection of wire mesh to RC frame

in all RC frame specimens, had the same mix design. The material tests of concrete and steel were performed according to the JIS [10]. The joint mortar consisted of cement and sand with mixing ratio of 1:2.5 and w/c is 0.40 for both specimens. The computation of masonry prism compressive strength was in compliance with ASTM C1314 [11]. From Table 4, it is evident that mortar strength of two specimens are different, the larger mortar strength of specimen IM-FC results in the increase of prism compressive strength. The Ferro-cement mortar consisted of cement and sand ratio of 1:3 with w/c is equal 0.45. The compressive strength of the mortar and tensile strength of wire mesh of the Ferro-cement are 23MPa and 420MPa, respectively.

3.3 Instrumentation and Loading

Both specimens were subjected to cyclic lateral loading and 200kN constant vertical loads on each column. The schematic diagram of the loading system is shown in Fig. 4, where two pantographs have been used to avoid any out-of-plane movement of the frame during loading. The cyclic lateral loading program consisted of two cycles for each lateral drift of 0.05, 0.1, 0.2, 0.4, 0.6, 0.8, 1.0, 1.5, and 2.0 %. The lateral drift is defined as the ratio of the top lateral displacement, measured at the center of beam, to the height of column taken from the top of the foundation beam to center of top beam. The

Table 2 Properties of concrete

Specimen	$f_{c'}$ (MPa)	E (MPa)	f_t (MPa)
IM	24.2	23000	2.1
IM-FC	24.9	24900	2.1

$f_{c'}$= Compressive strength, E= Elastic modulus and f_t= Split tensile strength

Table 3 Properties of steel reinforcement

Specimen	D6		D10	
	f_y (MPa)	f_{ult} (MPa)	f_y (MPa)	f_{ult} (MPa)
IM	480	675	350	559
IM-FC	476	595	384	547

f_y = yield strength and f_{ult} = ultimate strength

Table 4 Properties of masonry

Specimen	Brick	Masonry Prism			Mortar
	f_b (MPa)	f_{mas} (MPa)	E (MPa)	ε_{peak} (μ)	f_{mortar} (MPa)
IM	38.1	17.3	7840	3700	20.2
IM-FC	41.6	27.3	8725	3713	32.0

f_b= Compressive strength of brick, f_{mas}= Compressive strength, E= Elastic modulus and ε_{peak}= Strain at peak strength

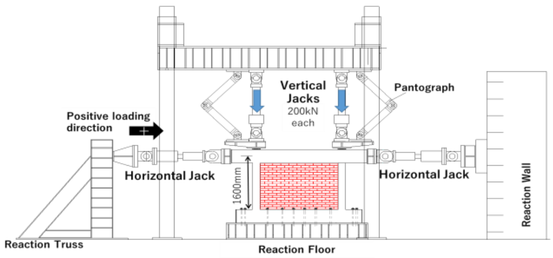

Fig. 4 Schematic diagram of loading system

average lateral top displacement has been recorded using LVDTs attached at the center of top beam. Several displacement transducers have also been attached over the height of RC columns to calculate column curvature. The internal local strains of column reinforcements have also been recorded using strain gauges attached on them.

4. EXPERIMENTAL RESULTS

4.1 Cyclic behavior under lateral load

(1) Infilled Masonry

The hysteresis behavior of infilled masonry is portrayed in Fig. 5(a). The response was linear up to the formation of first crack on mortar bed joint and diagonal cracks on brick near loading corner at 0.05% lateral drift. The long reinforcement of tension column yielded at above mid-height and upper critical section around 0.2% and 0.4% lateral drift. After approaching to maximum resistance at about 0.8% lateral drift, a sudden drop has been observed with extensive cracking on the masonry infill. After that, the masonry infilled RC frame started to sustain about 53% of its capacity up to 2% lateral drift. Loading has been postponed after 2% lateral drift of negative cycle as compression column reinforcement buckled which is followed by concrete spalling. The final state of cracks under positive and negative loading is shown in Fig. 6(a).

(2) Ferro-cement laminated infilled masonry

The hysteresis loops for Ferro-cement laminated infilled masonry is shown in Fig. 5(b). The response was essentially linear up to the formation of first crack on tension column at 0.05% lateral drift. At lateral drift of 0.1%, all longitudinal reinforcements yielded at the bottom of tension column. The yielding of reinforcement has been checked by strain that has been recorded by strain gauges. After cracking, the hysteresis loops began to open, specifically at the cycle of 0.4% lateral drift in which specimen reached to its maximum capacity and cracks occurred on the Ferro-cement laminated masonry. At around 0.6% drift, wire meshes started to be broken in tension which leads to sudden drop in lateral resistance of FC laminated infilled masonry. After that, the FC laminated RC frame started to sustain about 75% of its capacity up to 2% lateral drift. At about drift of 1%, lateral drift, the top column reinforcement bended, and sliding of the top beam with respect to laminated masonry has been observed. Loading has been postponed at the 1st cycle of negative 2% lateral drift, where the bottom reinforcement of compression column buckled which is followed by concrete spalling. The final crack pattern under positive and negative loading is shown in Fig. 6(b).

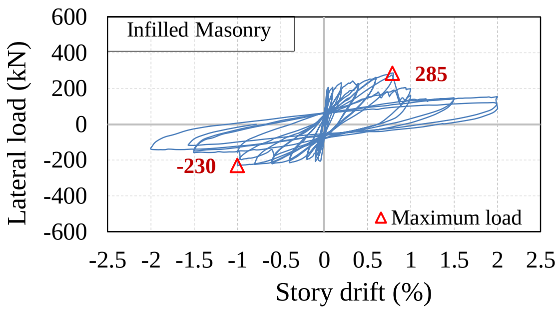

(a)

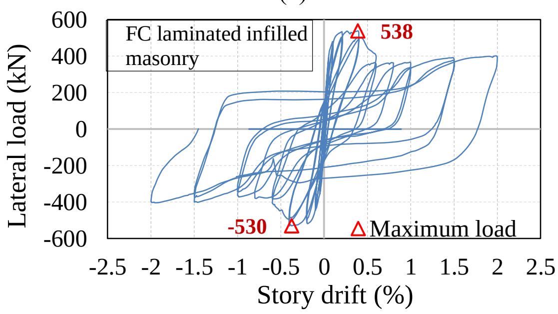

(b)

Fig. 5 Hysteresis curve of (a) Infilled masonry and (b) Ferro-cement laminated infilled masonry under lateral load

5. DISCUSSION ON EXPERIMENTAL RESULTS

5.1 Failure mechanism

The failure mode of structural wall, under lateral load, is mainly governed by shear, flexure or the combination of shear-flexure. To separate the contribution of flexure and shear in top displacement, the LVDTs attached on RC columns have been utilized to compute the flexural component of total story deformation. This is followed by the determination of

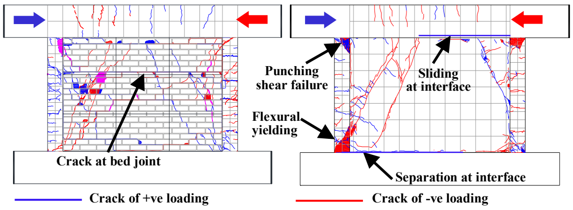

(a) (b)

Fig. 6 Crack pattern on (a) infilled masonry and (b) FC laminated infilled masonry at 2% story drift

shear deformation at a certain drift using Eq. 1.

$$\Delta_{total} = \Delta_{fl} + \Delta_{sh} \tag{1}$$

where, Δ_{total}, Δ_{fl}, Δ_{sh} refer to total, flexural and shear deformation, respectively at the center of beam. The contribution of flexural and shear component to total story deformation for both specimens, at selected lateral drift levels are shown in Fig. 7(a)-(b). In infilled masonry wall (IM), the contribution of flexural deformation is less than 20% throughout the courses of drift, as shown in Fig. 7(a), which implies a shear dominated failure that is also evident from the significant horizontal crack on the masonry as shown in Fig. 6(a). On the contrary, in Ferro-cement laminated masonry wall (IM-FC) the flexural contribution is more at initial stage as shown in Fig. 7(b), which indicates a flexure dominated failure that has also been confirmed from the flexural yielding at bottom of tension column and crack (i.e. separation) at the interface of retrofitted wall as shown in Fig. 6(b). From the failure mechanism, it is clear that Ferro-cement lamination improves the shear capacity of the overall frame which led to initiation of failure by flexure in retrofitted masonry infilled RC frame (IM-FC). The overall failure mechanism can be idealized as Fig. 8. At initial stage, nominal shear capacity (Q_{si}) is higher than flexural capacity (Q_{fl}) of the retrofitted wall. Gradually, the retrofitted wall experienced deterioration, due to onset of major cracks, which are thought to degrade the shear strength. On other words, after peak strength, the shear capacity became less than the flexural capacity which revoked the retrofitted wall to fail in shear (see Fig.8).

To evaluate this phenomenon, the flexural strength (at peak stage) and residual shear strength (post peak stage) of retrofitted RC frame has been computed as follows.

(1) Flexural shear capacity (Q_{fl})

The cracking mechanism of specimen IM-FC, at peak stage, is shown in Fig. 9(a). The flexural lateral capacity of the retrofitted frame has been computed using Eq. 2 and Eq. 3 as per JBDPA [12], which is generally used for concrete wall.

$$Q_{fl} = \frac{M_U}{h_o} \tag{2}$$

$$M_u = a_t . f_y . l_w + 0.5\sum(a_{wy} f_{wy}) . l_w + 0.5N . l_w \tag{3}$$

where, Q_{fl} = lateral capacity of the retrofitted wall considering flexural failure, M_u = ultimate moment

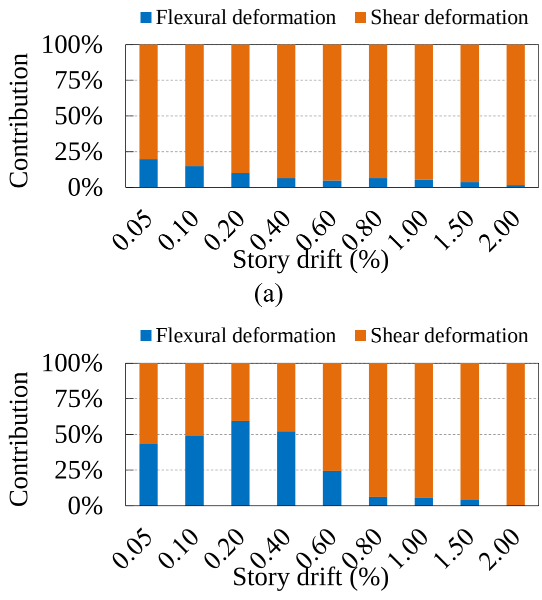

Fig. 7 Contributions of flexural and shear deformation of specimen (a) IM and (b) IM-FC

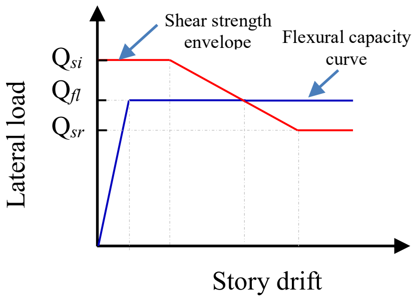

Fig. 8 Qualitative backbone curve of the retrofitted infilled masonry

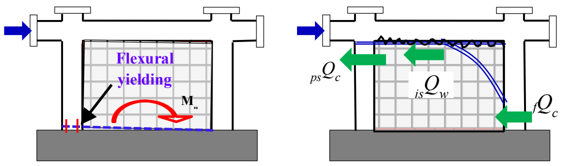

(a) (b)

Fig. 9 Free body diagram of retrofitted frame (IM- FC) at (a) peak and (b) post peak stage

capacity of the wall with boundary columns, h_o = clear height of wall, a_t, $\sum a_{wy}$ = cross sectional area of main bar in column and vertical reinforcing mesh reinforcement in wall, f_y, f_{wy} = yield strength of main bar and mesh reinforcement, N= total axial force in the boundary columns and l_w = center to center distance between boundary columns.

(2) Residual shear capacity (Q_{sr})

The schematic free body diagram of the retrofitted masonry infilled RC frame (IM-FC) at post peak stage is shown in Fig. 9(b). At post peak stage, the clear sliding along of infill along its attachment with upper beam has been observed. In addition, punching shear occurred at tension column, which can be computed as per JBDPA [12]. Therefore, the residual shear resistance (Q_{sr}) can be considered as Eq. 4 and computed from Eq. 5 to Eq. 7.

$$Q_{sr} = {}_{ps}Q_c + {}_{js}Q_w + {}_{f}Q_c \quad (4)$$

$$_{ps}Q_c = K_{min}\tau_o bD \quad (5)$$

$$_{js}Q_w = \sum a_{wm}\tau_y \quad (6)$$

$$_{f}Q_c = \frac{2M_c}{h_o} \quad (7)$$

where, $_{ps}Q_c$ = punching shear resistance of tension column, $_{js}Q_w$ = shear resistance provided by wire mesh, and $_{f}Q_c$= flexural shear resistance of compression column. M_c = flexural capacity of RC column, h_o = clear height of RC column, a_{wm} = area of wire reinforcement, τ_y = shear strength of wire, K_{min} = 0.34/(0.52+a/D), a= shear span = D/3, τ_o = shear strength of tension column, b and D = width and depth of column, respectively.

All of the computed values are shown in Table 5. From Fig. 10, it is evident that the flexural capacity without considering wire mesh give good approximation of lateral load capacity of FC retrofitted masonry infilled RC frame. However, the theoretical residual shear resistance can give a rough estimation of residual shear resistance.

5.2 Initial Stiffness

The envelope curve of both specimens are shown in Fig.11(a). The experimental initial stiffness, computed at 0.1% drift of the Ferro-cement laminated RC frame (IM-FC) is about 300 kN/mm, which is 2.3 times higher than that of masonry infilled RC frame (IM). The initial stiffness deterioration is shown in Fig.11(b), which indicates the similar stiffness deterioration of both specimens, with and without Ferro-cement lamination.

The initial stiffness can be evaluated considering the concept of diagonal strut where the initial stiffness is the summation of flexural stiffness of RC frame (K_f) and lateral stiffness of diagonal strut of infill panel (K_{inf}). The initial stiffness can be determined using Eq. 8 to Eq. 11.

$$K_{initial} = K_f + K_{\inf} \quad (8)$$

$$k_f = \frac{24E_c I_c}{h_c^3}\,\frac{12\rho+1}{12\rho+4} \quad (9)$$

$$k_{\inf} = \frac{E_{mas}W_{\inf}t_{\inf}\cos^2\theta}{d_{\inf}} \quad (10)$$

$$t_{\inf} = t_{mas} + 2t_{mor}\frac{E_{mor}}{E_{mas}} \quad (11)$$

where, K_{intial}= initial stiffness, K_f = flexural stiffness of RC frame, K_{inf} = stiffness of infill panel, E_c = young modulus of concrete, I_c = moment of inertia of column, h_c = column height, ρ = beam-column stiffness ratio, E_{mas} = young modulus of masonry, W_{inf} = width of diagonal strut, t_{inf} = equivalent thickness of Ferro-cement laminated masonry, d_{inf} = diagonal length of infill panel, θ = inclination of diagonal, t_{mas} = thickness of masonry, t_{mor} = thickness of Ferro-cement mortar, E_{mor} = young modulus of Ferro-cement mortar, respectively. In this study, diagonal strut width has been considered 0.25d_{inf} as prescribed by Paulay and Priestley [13].

The initial stiffness can also be estimated using the concept of composite section, which is generally used for masonry infilled RC frame, suggested by Fiorato et al. [14]. In this method, frame is considered as a composite beam, where RC columns are assumed as flanges and the infilled panel is assumed as web. The initial stiffness of the retrofitted masonry infilled RC frame has been estimated using Eq. 12 to Eq. 14.

$$K_{initial} = \frac{1}{\frac{1}{K_{fl}} + \frac{1}{K_{sh}}} \quad (12)$$

$$K_{fl} = \frac{3E_c I_{ce}}{h_c^3} \quad (13)$$

$$K_{sh} = \frac{(A_w G_w) + (A_m G_m)}{h_w} \quad (14)$$

where $K_{initial}$, K_{fl} and K_{sh} represent the initial, flexural and shear stiffness of the overall frame, respectively. E_c = young modulus of concrete, I_{ce} = equivalent moment of inertia of transformed section, h_c = column height, h_w = height of masonry wall, A_w/A_m = area of masonry/ Ferro-cement layer, and G_w/G_m = shear modulus of masonry wall/mortar, respectively.

The experimental and estimated initial stiffness of the both specimens (IM and IM-FC) are shown in Fig. 12. It is evident for both specimens (IM and IM- FC) that the diagonal strut assumption gave a good approximation of initial stiffness than composite section hypothesis.

5.3 Lateral Strength

The average peak resistance of both specimens are presented in Table 5. The Ferro-cement lamination on infilled masonry improved the lateral capacity of masonry infilled RC frame about 2 times with 0.16% horizontal mesh reinforcement, however the actual contribution of Ferro-cement to the strength could not be determined due to the differences in failure mode and material properties.

Table 5 Lateral capacity of specimens

Lateral capacity (kN)		Specimen	
		IM	IM-FC
Experimental	Peak (avg.)	257	534
	Residual (avg.)	-	373
Flexural capacity (w/ wire mesh)		-	627
Flexural capacity (w/o wire mesh)		-	551
Residual shear capacity		-	295

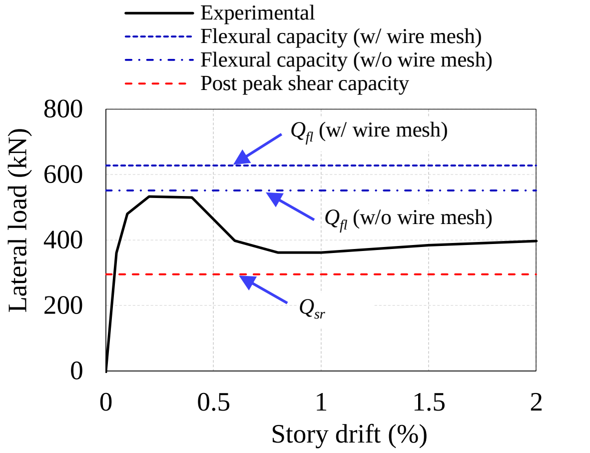

Fig. 10 Experimental backbone curve of the retrofitted infilled masonry with predicted capacity

5.4 Energy Dissipation

The average cumulative energy dissipated by infilled masonry (IM) and retrofitted infilled masonry (IM-FC) are shown in Fig. 13. It is evident from the energy dissipation that the Ferro-cement lamination on infilled masonry resulted in almost 2 times energy dissipation than that of in infilled masonry (IM).

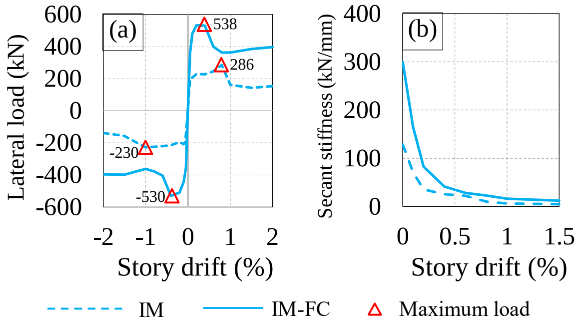

Fig. 11 (a) load-story drift envelope curve
(b) stiffness degradation curve

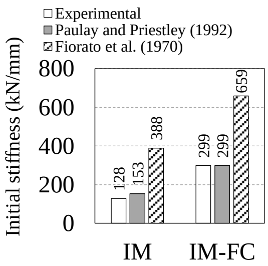

Fig. 12 Initial stiffness of specimens

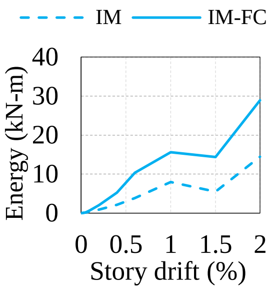

Fig. 13 Cumulative energy dissipation at different story drifts

6. CONCLUSIONS

In this study, an experimental investigation has been conducted on the overall behavior of infilled masonry and Ferro-cement laminated infilled RC frame. This is followed by the comparison of failure mechanism, lateral strength, dissipated energy of Ferro-cemented masonry with infilled masonry. The following conclusions can be drawn from this study-

1. Ferro-cement lamination on infilled masonry changed the shear dominated failure of masonry infilled RC frame to flexural failure.
2. The flexural capacity model adopted in JBDPA [12] for concrete wall can predict the lateral capacity of Ferro-cement laminated masonry infilled RC frame.
3. The diagonal strut concept can predict the initial stiffness of Ferro-cement laminated infilled masonry.
4. Ferro-cement lamination on infilled masonry, with 0.16% mesh reinforcement, increased the lateral strength, initial stiffness, and energy dissipation about 2, 2.3 and 2 times, respectively.

Even though Ferro-cement retrofitted specimen showed good improvement in lateral strength, however, it should be noted that direct comparison of improvement in lateral strength by Ferro-cement needs further investigation because of the differences in failure mode as well as material properties of the both specimens in this study.

ACKNOWLEDGEMENT

This research is supported by SATREPS project lead by Prof. Nakano Yoshiaki, U. Tokyo and JSPS KAKENHI Grant Number JP18H01578 (Principal investigator: Prof. Masaki Maeda, Tohoku University). Authors would like to acknowledge the cordial help of Ms. Tafheem, Mr. Hashib and Mr. Jobaer in experimental work. The discussion and guidance by Dr. Matsutaro Seki, BRI has been greatly acknowledged.

REFERENCES

[1] Balaguru, P. N., and Soroushian, P.: State-of-the-art Report on Ferrocement, ACI Committee, 549R-97, 1997

[2] Kaya, F., Tekeli, H., and Anil, Ö.: Experimental behavior of strengthening of masonry infilled RC frames by adding rebar-reinforced stucco, Struc. Conc., pp. 1-14, 2018.2

[3] Seki, M., Popa, V., Lozinca, E., Dutu, A., and Papurcu, A.: Experimental study on retrofit technologies for RC frames with infilled brick masonry walls in developing countries, In Proceedings of the 16th ECEE, Romania, 2018.6

[4] Demirel, I. O., Yakut, A, Binici, B. and Canbay, E.: An Experimental Investigation of Infill Behaviour in RC Frames, In Proc. of the 10th PCEE, Australia, 2015.11

[5] Altın, S., Anıl, Ö., Kopraman, Y., and Belgin, Ç.: Strengthening masonry infill walls with reinforced plaster, In Proc. of the Institution of Civil Engineers-Structures and Buildings, 163, pp. 331-342, 2010

[6] Calvi, G. M., & Bolognini, D.: Seismic response of RC frames infilled with weakly reinforced masonry panels, Jour. of Earthq. Engg., Vol. 5, pp. 153-185, 2001

[7] Alcocer, S. M., Ruiz, J., Pineda, J. A., and Zepeda, J. A.: Retrofitting of confined masonry walls with welded wire mesh, In Proc. of the 11th WCEE, 1996.6

[8] Žarnić, R., and Tomaževič, M.: Behaviour of masonry infilled RC frames subjected to seismic loading, 1985.

[9] Alwashali, H., Torihata, Y., Jin, K., and Maeda, M. (2018). Experimental observations on the in-plane behaviour of masonry wall infilled RC frames; focusing on deformation limits and backbone curve. Bulletin of Earthquake Engineering, 16(3), 1373-1397.

[10] Japanese Standard Association. Jap. Industrial Standards. 2010 (No. JIS R1250, JIS Z 2201, JIS A 1108, JIS A 1113).

[11] American Society of Testing and Materials (ASTM). Standard test method for compressive strength of masonry prisms. 2011 (ASTM C1314)

[12] Japan Building Disaster Prevention Association, Standard for seismic evaluation of existing conc. Buildings, 2001

[13] Paulay, T. and Priestley, M.J.N. (1992) Seismic design of RC and masonry buildings. Wiley,New York

[14] Fiorato, A.E., M.A. Sozen, and W.L. Gamble (1970). "An investigation of the interaction of RC frames with masonry filler walls." Report No. UILU-ENG 70-100, University of Illinois at Urbana-Champaign.